# RESPONSE ANALYSIS METHOD OF TRADITIONAL WOODEN STRUCTURE PLACED FREE ON FOUNDATION

**T. Kawakami [1], K. Mukaibo [2] and Y. Suzuki [3]**

[1] *Staff, TAKENAKA Corporation, Osaka, Japan*

[2] *Researcher, Kyoto University, Kyoto, Japan*

[3] *Professor, Ritsumeikan University, Shiga, Japan*

*Email: kawakami.takuma@takenaka.co.jp, mukaibou@zeisei.dpri.kyoto-u.ac.jp, suzuki-y@fc.ritsumei.ac.jp*

**ABSTRACT:**

In this paper, a method of response analysis for traditional wooden structures is presented. Their columns are just placed and not fastened on foundations. Sliding and rotating behaviors in addition to shear deformation of wooden frame occur during earthquakes, and they are then considered in the analysis. The effects of impact between columns and foundations are also taken into account. Necessary conditions for occurrences of sliding and rotating are examined, and two-dimensional equations of motion are formulated. In order to verify the proposed method, shaking table tests were carried out. First, the analytical results for sliding response of a short and rigid wooden frame model without shear deforming and rotating under horizontal excitation show good agreement with the results of shaking table tests. Secondly the analytical results for shear deforming, rotating and sliding responses of a full-scale wooden frame agree well with the experimental results. It is found that the proposed analytical method can comprehend the special behaviors including sliding and rotating of traditional wooden structures under earthquakes.

**KEYWORDS:** Traditional wooden building, Sliding, Rotating, Shaking table test, Response analysis

## 1. INTRODUCTION

In many of traditional wooden buildings in Japan, columns are often placed free on stone foundations without using ground sills. Since the bottom of column is not fixed to the ground, these wooden buildings have possibility of sliding and rotating during severe earthquake motions. In evaluating the seismic safety of a whole building, it is necessary to take account of these behaviors. Many researchers have investigated the sliding, rocking and overturning of rigid bodies. For example, Ishiyama (1982) classified the motions of rigid bodies into six types: rest, slide, rotation, slide rotation, translation jump and rotation jump, and investigated the characteristics of motions and overturning of rigid bodies numerically. As for a traditional wooden frame, the seismic response includes the shear deformation of walls, and the response characteristics considerably differ from those of rigid bodies. The influences of the sliding and rocking behaviors on the seismic performance of a whole building have not been clarified yet. The objectives of this paper are to develop an analysis method considering those seismic behaviors and to verify its validity based on shaking table tests.

## 2. SHAKING TABLE TESTS

### *2.1 Outline*

Testing specimens were two types of wooden frames, as shown in Figure 1. Their dimensions were 1,820mm×1,820mm in plan. The height of the specimen L was 570mm, and that of the specimens H was 2,560mm. A dry-mud wall panel (Sugiyama et al. 2006) was adopted as a seismic resisting shear wall for the specimen H, and wooden connections were constructed without using any metal devices. The specimens were just placed on the base stone foundations which were fixed on the shaking table. The dimension of the base stone is 500mm×500mm in plan and 60mm in thickness. As the dead load, a square steel plate was mounted on the top of the specimens. The weights of the steel plates were 3.0, 4.0, and 5.0tonf. Consequently, six types of specimens were tested. Table 2.1 shows the names of specimens and their total weights. For example, L3 means

the specimen L with 3.0tonf steel weight. The base shear coefficients of the specimen H3, H4, and H5 are 1.10, 0.81, and 0.66, respectively.

As input ground motions, sinusoidal waves at 1.0Hz and 2.0Hz, and the artificial earthquake wave simulated by Building Center of Japan (BCJ-L2) were input in the X-direction. Their acceleration amplitudes were adjusted to various intensities. Accelerometers were installed on the top of the steel weight and on the shaking table. Strains of columns and beams were measured by strain gages. Absolute and relative displacements were also measured at various locations.

Table 2.1 Total weight of specimens

| Specimen | L3 | L4 | L5 | H3 | H4 | H5 |
|---|---|---|---|---|---|---|
| Weight[kN] | 31.4 | 41.2 | 51.1 | 32.3 | 42.1 | 51.9 |


a) Specimen L b) Specimen H

Figure 1 Schematic drawings of testing specimens

*2.2 Result of Specimen L*

*2.2.1 Sliding behavior*

Figure 2 shows the residual sliding displacement when BCJ-L2 wave and sin 1.0Hz were input. Plotted points with asterisks in Figure 2b denote the results obtained when the input time duration was different from others. In the case of BCJ-L2 wave, the residual displacement increased in proportion to the input acceleration amplitude. In the case of sin 1.0Hz, however, the relation between the residual displacement and the input amplitude was not always proportional.

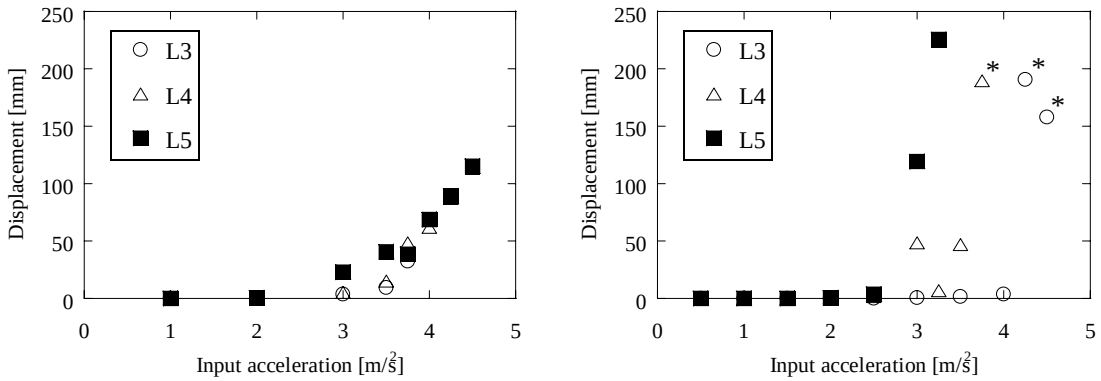


a) BCJ-L2 wave b) sin 1.0Hz wave

Figure 2 Residual sliding displacements after each excitation

Figure 3 shows the time history of the sliding displacement of the specimen L5 subjected to sinusoidal waves of the maximum acceleration 3.25m/s$^2$. In the case of sin 1.0Hz, the specimen slid to only the negative direction. On the other hand, in the case of sin 2.0Hz, the specimen slid to both the directions. The difference of these sliding behavior resulted in the residual displacement.

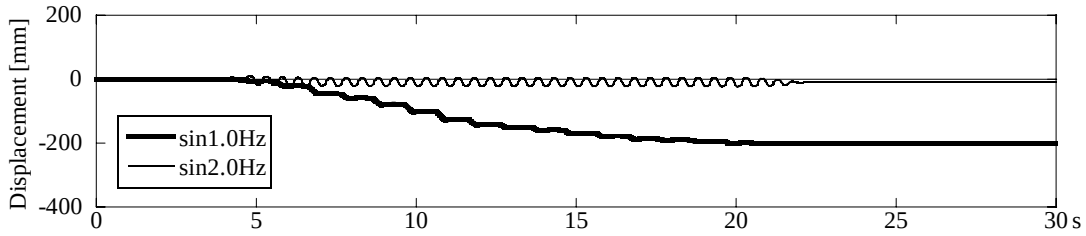


Figure 3 Time history of sliding displacement of specimen L5 of the maximum input acceleration 3.25m/s$^2$

*2.1.2 Static friction coefficient*

Table 2.2 shows the average values of friction coefficients, calculated by using the instantaneous response accelerations and vertical axial loads at slidings. The sliding instants were identified from the time histories of the sliding displacements and videos during the tests.

Table 2.2 Average values of friction coefficient

| L3 | L4 | L5 | Ave. |
|---|---|---|---|
| 0.40 | 0.40 | 0.33 | 0.38 |

*2.2 Result of Specimen H*

*2.2.1 Sliding and rotating behavior*

Figure 4 shows the response displacement of the specimen H3 subjected to BCJ-L2 wave adjusted to the maximum acceleration 2.0m/s$^2$. The thick gray line denotes the relative displacement of the column top, and the black line denotes that of the column bottom, that is, the sliding displacement. The vertical dotted lines denote the time instants when the rotation of the specimen occurred. It is found that the vibrational behavior of the specimen consists of the shear deformation, sliding, and rotation.

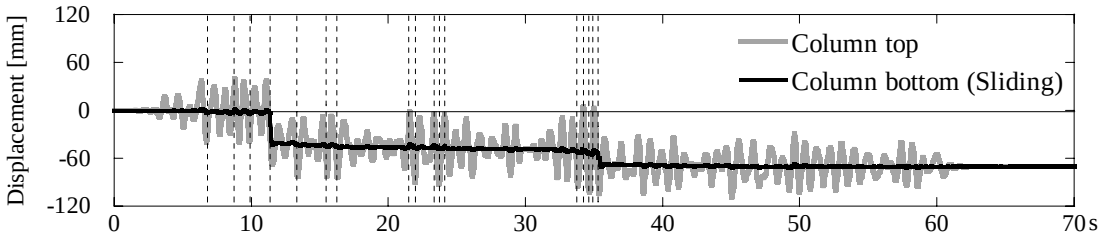


Figure 4 Response displacement of specimen H3 subjected to BCJ-L2 wave 2.0m/s$^2$

*2.2.2 Response acceleration during rotation*

Figure 5a shows the response acceleration of the column top of the specimen H3 subjected to sin 1.0Hz of the maximum acceleration 2.5m/s$^2$. The large rotating behaviors occurred in time zones denoted by arrows. The acceleration peaks were observed in the beginning and the end of each time zone, and the specimen vibrated at high frequency in the time zone. In changing from one time zone to the next, the sudden change of the response acceleration in the opposite direction was observed.

*2.2.3 Bending moment on column during rotation*

Figure 5b shows the bending moment affected on the column. During each time zone denoting the rotating behavior, the bending moment was almost constant. Therefore, it is found that the specimen during the rotation keeps its shape of deformation.

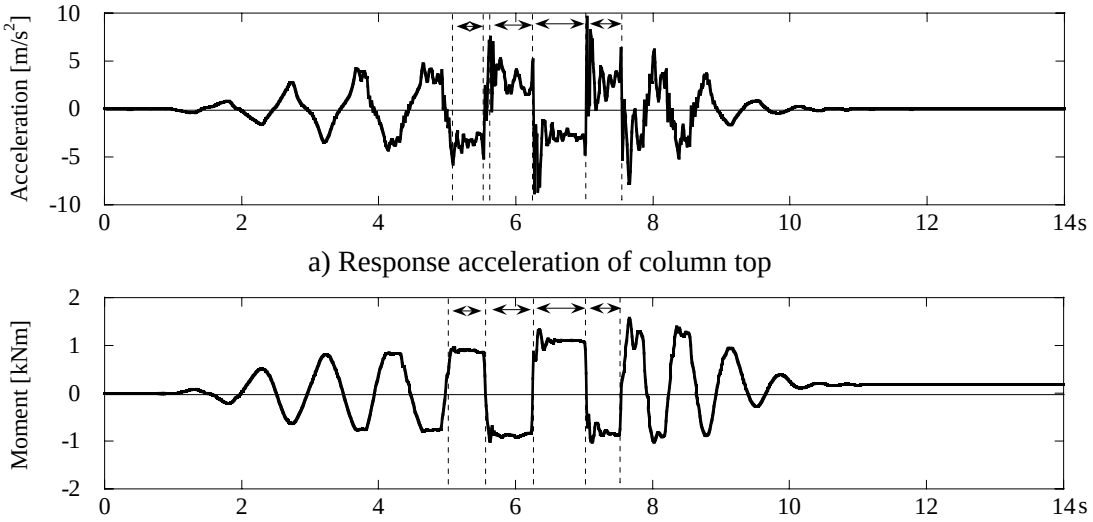


a) Response acceleration of column top

b) Bending moment on column

Figure 5 Response of specimen H3 subjected to sin 1.0Hz 2.50m/s$^2$

*2.2.4 Vertical response caused by collision between column and base stone*

Figure 6a shows an enlarged view of Figure 5a, and Figure 6b shows the variation of the vertical axial load. From Figure 6b, it is found that the large compressive force, which was greater than 50kN, occurred in the vertical direction at the end of the rotation. This was due to the collision between the column and base stone. The time history of the vertical axial load after the collision is similar to a free vibrational response of a single-degree-of-freedom system by an impulsive force. As no external force was input in the vertical direction, the axial deformation of the columns may be interpreted as a cause of this free vibration.

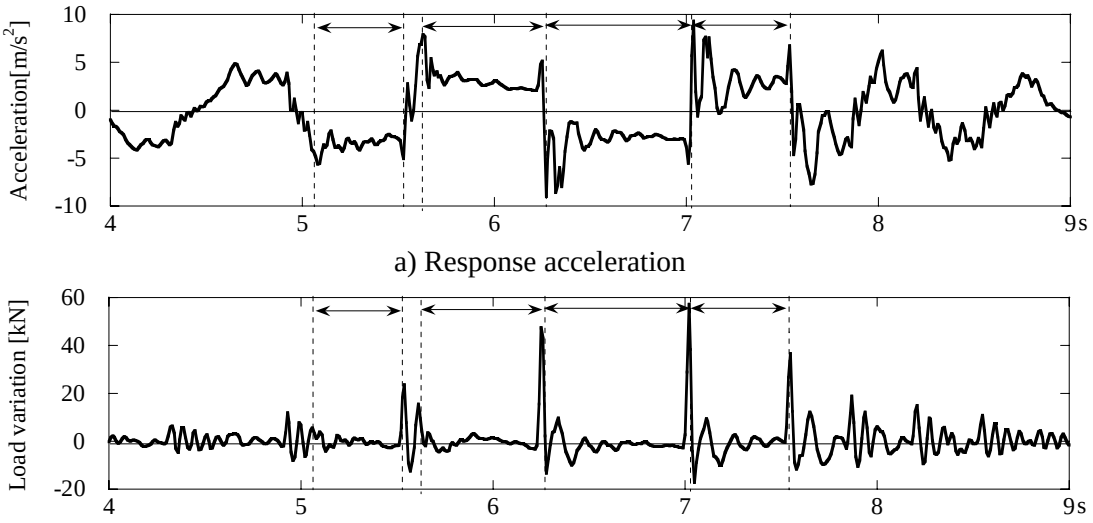


a) Response acceleration

b) Variation of vertical axial load

Figure 6 Response of specimen H3 subjected to sin 1.0Hz 2.50m/s$^2$

## 3. NUMERICAL ANALYSIS METHOD

*3.1 Assumptions*

In a numerical analysis, assume as follows:

1) The sliding behavior at the column bottom obeys Coulomb's rule.
2) The rotation of the wooden frame begins when the axial force at the column bottom becomes zero.

3) The wooden frame keeps its shape of deformation during rotation.
4) The velocity vector of gravity point of the frame does not change by collisions between column and base stone.

*3.2 Equations of Motion*

The shear deformation of the wooden frame, sliding, and rotation in the vertical plane are modeled in a complex plane as shown in Figure 7. Here, $m$ and $m_s$ are masses, where $m_s$ is much smaller than $m$, $I$ is the inertia moment, and $h$ and $b$ are the height and half width. $\mathbf{w}_g$ is the displacement vector of ground motion, and $\mathbf{w}_d$, $\mathbf{w}_r$ are displacement vectors of the gravity point due to shear deformation, rotation, respectively, and, $\mathbf{w}_s$ is the displacement vector of sliding.

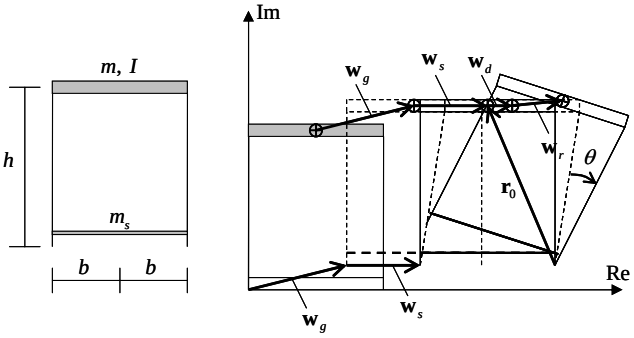


Figure 7 Analysis model

The absolute displacement $\mathbf{w}$ of gravity point in the frame is then given by

$$\mathbf{w} = \mathbf{w}_d + \mathbf{w}_r + \mathbf{w}_s + \mathbf{w}_g \tag{3.1}$$

The rotational angle $\theta$ is related to $\mathbf{w}_d$ and $\mathbf{w}_r$:

$$(\mathbf{r}_0 + \mathbf{w}_d)e^{i\theta} = \mathbf{r}_0 + \mathbf{w}_d + \mathbf{w}_r \tag{3.2}$$

where $\mathbf{r}_0$ is a constant vector between the gravity point and a supporting point of rotation at $\mathbf{w}_d = 0$. By using Eqs. 3.1 and 3.2, the velocity and acceleration vectors are obtained:

$$\dot{\mathbf{w}} = i\dot{\theta}(\mathbf{r}_0 + \mathbf{w}_d)e^{i\theta} + \dot{\mathbf{w}}_d e^{i\theta} + \dot{\mathbf{w}}_s + \dot{\mathbf{w}}_g \tag{3.3}$$

$$\ddot{\mathbf{w}} = (i\ddot{\theta} - \dot{\theta}^2)(\mathbf{r}_0 + \mathbf{w}_s)e^{i\theta} + 2i\dot{\theta}\dot{\mathbf{w}}_d e^{i\theta} + \ddot{\mathbf{w}}_d e^{i\theta} + \ddot{\mathbf{w}}_s + \ddot{\mathbf{w}}_g \tag{3.4}$$

The equations of motion of shear deformation are

$$\mathrm{Re}\{m\ddot{\mathbf{w}}_d\} + c_x \mathrm{Re}\{\dot{\mathbf{w}}_d\} + k_x \mathrm{Re}\{\mathbf{w}_d\} = -\mathrm{Re}\{m\ddot{\mathbf{w}}_g\} \tag{3.5}$$

$$\mathrm{Im}\{m\ddot{\mathbf{w}}_d\} + c_y \mathrm{Im}\{\dot{\mathbf{w}}_d\} + k_y \mathrm{Im}\{\mathbf{w}_d\} = -\mathrm{Im}\{m\ddot{\mathbf{w}}_g\} \tag{3.6}$$

where Re{ } and Im{ } are real and imaginary parts of { }, respectively. $k_x$ and $k_y$ are stiffness in the horizontal and vertical direction, respectively. $c_x$ and $c_y$ are damping coefficients. By considering two degree-of-freedom system, the equations of motion of sliding are obtained:

$$\begin{bmatrix} m_s & 0 \\ 0 & m \end{bmatrix}\begin{Bmatrix} \mathrm{Re}\{\ddot{\mathbf{w}}_s\} \\ \mathrm{Re}\{\ddot{\mathbf{w}}_d + \ddot{\mathbf{w}}_s\} \end{Bmatrix} + \begin{bmatrix} c_x & -c_x \\ -c_x & c_x \end{bmatrix}\begin{Bmatrix} \mathrm{Re}\{\dot{\mathbf{w}}_s\} \\ \mathrm{Re}\{\dot{\mathbf{w}}_d + \dot{\mathbf{w}}_s\} \end{Bmatrix} + \begin{bmatrix} k_x & -k_x \\ -k_x & k_x \end{bmatrix}\begin{Bmatrix} \mathrm{Re}\{\mathbf{w}_s\} \\ \mathrm{Re}\{\mathbf{w}_d + \mathbf{w}_s\} \end{Bmatrix} + \begin{Bmatrix} F_s \\ 0 \end{Bmatrix} = -\begin{Bmatrix} m_s \\ m \end{Bmatrix}\mathrm{Re}\{\ddot{\mathbf{w}}_g\} \tag{3.7}$$

$$\mathrm{Im}\{m\ddot{\mathbf{w}}_d\} + c_y \mathrm{Im}\{\dot{\mathbf{w}}_d\} + k_y \mathrm{Im}\{\mathbf{w}_d\} = -\mathrm{Im}\{m\ddot{\mathbf{w}}_g\} \tag{3.8}$$

where $F_s$ is a friction force given by

$$F_s = \mathrm{sgn}(\mathrm{Re}\{\dot{\mathbf{w}}_s\})\mu'(m + m_s)\mathrm{Im}\{\ddot{\mathbf{w}}_d + \ddot{\mathbf{w}}_g + ig\} \tag{3.9}$$

where sgn is the signum function, $\mu'$ is the dynamic friction coefficient, and $g$ is the gravitational acceleration. By considering moment equilibrium, the equations of motion of rotation are obtained:

$$I\ddot{\theta} + \mathrm{Re}\{m\mathbf{s}\bar{\mathbf{s}}\ddot{\theta}\} = \mathrm{Re}\{m\bar{\mathbf{s}}(i\ddot{\mathbf{w}}_g - g)(1 - i\theta)\} \tag{3.10}$$

where $\mathbf{s} = \mathbf{r}_0 + \mathbf{w}_{d0}$, and $\mathbf{w}_{d0}$ is a displacement vector due to shear deformation at the beginning of rotation. $\bar{\mathbf{s}}$ is the complex conjugate of $\mathbf{s}$. The equations of motion of sliding during rotation are given by

$$I\ddot{\theta} + \mathrm{Im}\left\{ m\left(-\mathrm{sgn}\left(\dot{\mathbf{w}}_s\right)\mu' + i\right)\mathrm{Im}\left\{ i\mathbf{s}\right\}\bar{\mathbf{s}}\ddot{\theta}\right\}$$
$$= -\mathrm{Im}\left\{ m\left(-\mathrm{sgn}\left(\dot{\mathbf{w}}_s\right)\mu' + i\right)\mathrm{Im}\left\{ \ddot{\mathbf{w}}_g + ig\right\}\bar{\mathbf{s}}\right\} + \mathrm{Im}\left\{ m\left(-\mathrm{sgn}\left(\dot{\mathbf{w}}_s\right)\mu'\mathrm{Im}\left\{ \ddot{\mathbf{w}}_g + ig\right\}\bar{\mathbf{s}}\right)i\theta\right\} \tag{3.11}$$

*3.3 Necessary conditions*

Necessary conditions for shear deformation, sliding and rotation are described by the input and the response value. As criteria, two values, $S$ and $R$, which are related to sliding and rotation, respectively, are defined as follows:

$$S = \mu\,\mathrm{Im}\left\{ \ddot{\mathbf{w}} + ig\right\}, \quad R = \frac{1}{h}\left\{ b - \mathrm{sgn}\left(\mathrm{Re}\{\mathbf{w}_d\}\right)\mathrm{Re}\left\{ \mathbf{w}_d\right\}\right\}\mathrm{Im}\left\{ \ddot{\mathbf{w}} + ig\right\} \tag{3.12}$$

For example, Eqs. 3.5 and 3.6 govern the motion of the frame if

$$\left|\mathrm{Re}\left\{\ddot{\mathbf{w}} + ig\right\}\right| \le S \ , \ \left|\mathrm{Re}\left\{\ddot{\mathbf{w}} + ig\right\}\right| \le R \tag{3.13}$$

## 4. ANALYSIS RESULT

*4.1 Analytical Model for Specimen L*

The restoring force characteristic of the specimen L is modelled as a bi-linear hysteresis as shown in Figure 8 and the model parameters are chosen based on the test results. Table 4.1 shows the model parameters for the specimen L. As the friction coefficient, the values shown in Table 2.2 are adopted. Figure 9 shows the comparisons of sliding displacement between the analytical and the experimental results. The analytical results show good agreement with the experimental results.

Table 4.1 Numerical parameters of model L

| Specimen | $m$ [kN] | $m_s$ [kN] | $b$ [m] | $h$ [m] | $a$ [kN] | $k_1$ [kN/mm] | $k_2$ [kN/mm] | Damping factor |
|---|---|---|---|---|---|---|---|---|
| L3 | 31.2 | 0.3 | 0.91 | 0.57 | 3.0 | 18.8 | 2.0 | 0.05 |
| L4 | 41.2 | | | | | 17.9 | 2.0 | |
| L5 | 51.1 | | | | | 18.2 | 2.0 | |

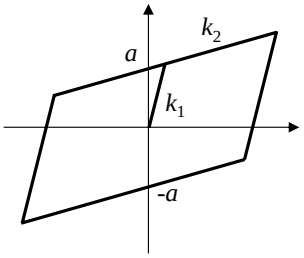


Figure 8 Restoring force of model L

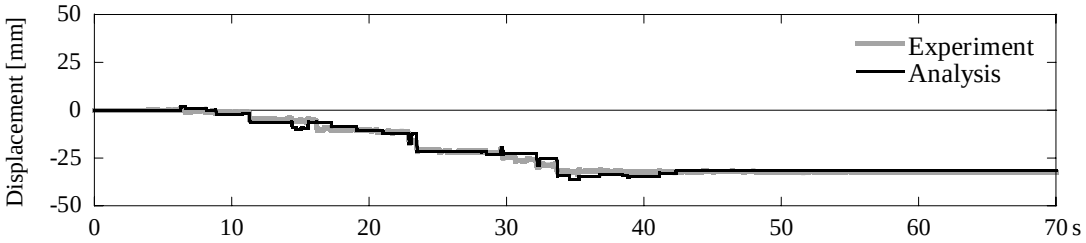


a) Sliding displacement of L3 subjected to BCJ-L2 wave 3.75m/s$^2$

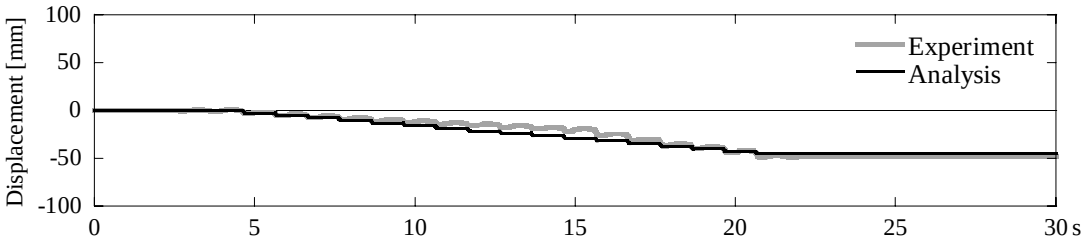


b) Sliding displacement of L4 subjected to sin 2.0Hz wave 3.0m/s$^2$

Figure 9 Comparisons of sliding displacement between analytical and experimental results for specimen L

*4.2 Analytical Model for Specimen H*

Table 4.2 shows the model parameters for the specimen H3. The restoring force characteristic is modeled as shown in Figure 10 and the model parameters are chosen based on the test results. The friction coefficient is 0.336 in the case of BCJ-L2 wave input, and 0.345 in the case of sinusoidal wave input. The vertical stiffness of the model is 10.68kN/mm, which is determined by Young's modulus of columns. Figure 11 shows the comparison of the response acceleration, relative displacement, and vertical axial load. In Figure 11b, some of the experimental data is missing at about 6.5s ~ 7.0s because the displacement of the frame exceeded the measurable limit. The analytical results show good agreement with the experimental ones.

Table 4.2 Numerical parameters of model H

| Specimen | $m$ [kN] | $m_s$ [kN] | $b$ [m] | $h$ [m] | | |
|---|---|---|---|---|---|---|
| H3 | 32.3 | 1.42 | 0.91 | 2.56 | | |
| Input wave | $k_1$ [kN/mm] | $k_2$ [kN/mm] | $k_3$ [kN/mm] | $a$ [kN] | $c$ [mm] | Damping factor |
| BCJ-L2 | 1.0 | 0.13 | 0.35 | 0.5 | 0.015 | 0.010 |
| sin 1.0Hz | 2.0 | 0.45 | 1.00 | 1.0 | 0.015 | 0.015 |

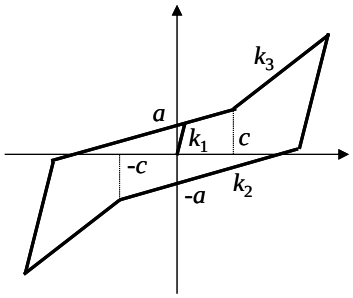


Figure 10 Restoring force of model H

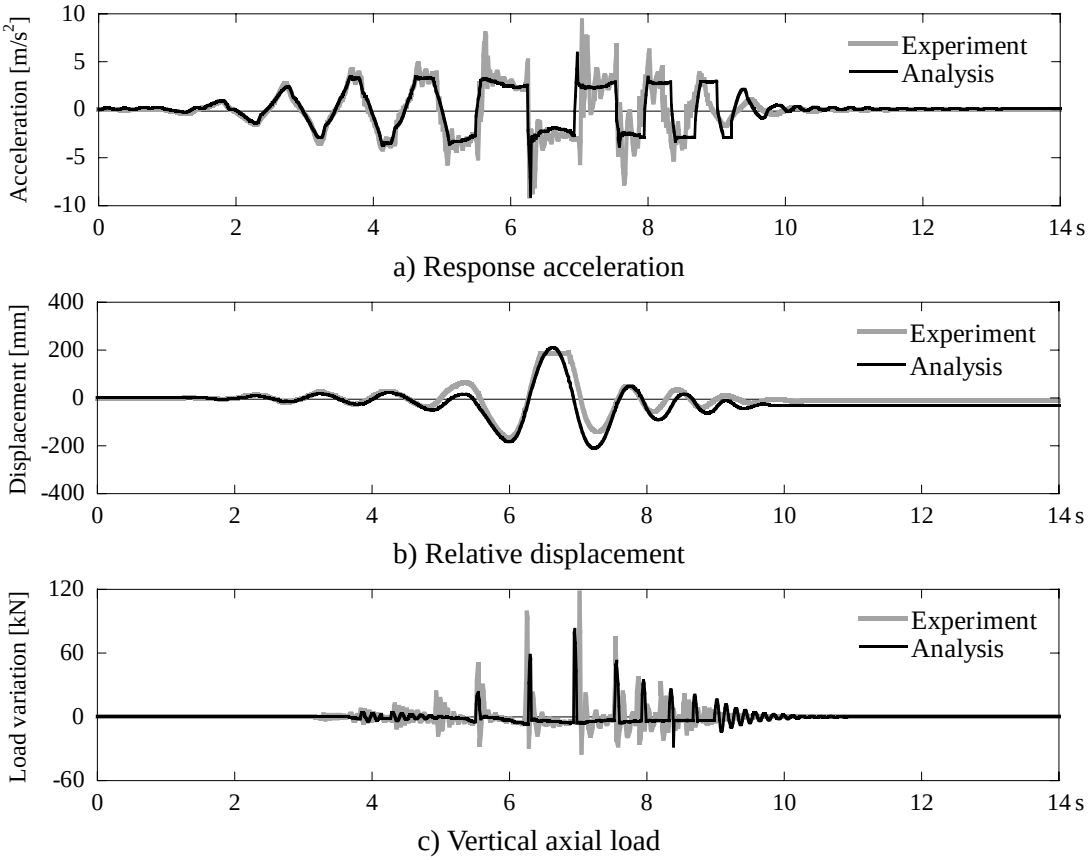


a) Response acceleration

b) Relative displacement

c) Vertical axial load

Figure 11 Comparison of responses between analytical and experimental results for H3 subjected to sin 1.0Hz 2.5m/s$^2$

Figure 12 shows analytical results of the relative displacement for the specimen H under different assumptions. Figure 12a shows the result when the model is forced not to deform. In Figure 12b, a black line denotes the result when the model is forced not to rotate, a dotted line denotes the result when a model is forced not to slide, and a gray line denotes the result already shown in Figure 11b. It is found that if any motion state of a model is ignored, the analytical results do not agree with the testing results.

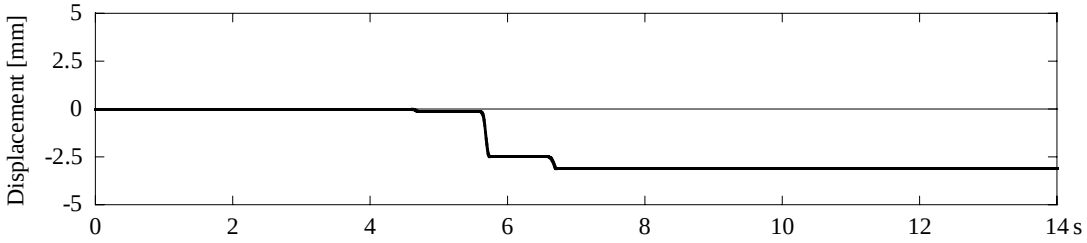


a) Forced not to deform (rigid body)

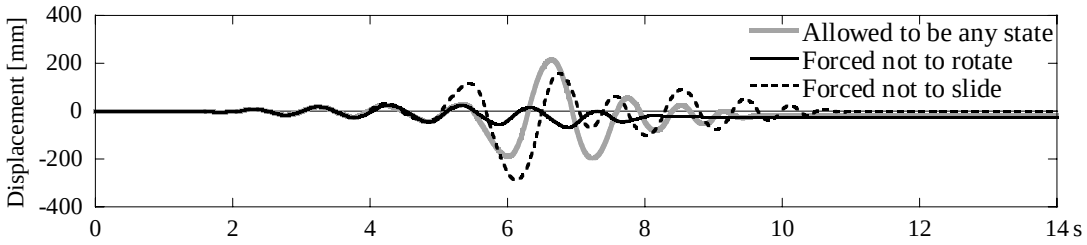


b) Forced not to rotate and not to slide

Figure 12 Comparisons of relative displacement under different assumptions for specimen H3

## 5. CONCLUSION

In this study, a method of response analysis for traditional wooden structures is developed by considering sliding and rotating behaviors in addition to shear deformation of wooden frame, and its validity is verified based on the shaking table test. The analytical results show good agreement with the test results. The proposed analysis method is capable of simulating the seismic behavior of traditional wooden structures. However, the extension of this method to more realistic buildings is needed in the future research.

## ACKNOWLEDGMENTS

This research was partially supported by the Grant-in-Aid for Scientific Research (S) under Project No. 19106010 sponsored by the Japanese Ministry of Education, Culture, Sports, Science and Technology. The vibration tests of wooden frames were conducted by using a shaking table at the Disaster Prevention Research Institute (DPRI), Kyoto University, Japan.

## REFERENCES

Ishiyama, Y., (1982), Motions of Rigid Bodies in Response to Earthquake Excitations – Equations of Motions and Computer Simulation, *Transactions of the Architectural Institute of Japan*, **314**, 33-47.
Sugiyama, R., Suzuki, Y., Gotou, M., and Murakami, H., (2006), Development of Bearing Wall for Timber Frame by Using Dry Mud-panels, *AIJ Journal of Technology and Design*, **24**, 125-130. (in Japanese)